Biotechnology and Bioprocess Engineering 27: 202-212 (2022)
DOI 10.1007/s12257-021-0220-0

pISSN 1226-8372
eISSN 1976-3816

RESEARCH PAPER

# Rolling Circle Amplification-based Copper Nanoparticle Synthesis on Cyclic Olefin Copolymer Substrate and Its Application in Aptasensor

**Tai-Yong Kim, Min-Cheol Lim, Ji Won Lim, and Min-Ah Woo**

Received: 5 August 2021 / Revised: 16 September 2021 / Accepted: 19 September 2021


**Abstract** This study aimed to develop a label-free fluorescent aptasensor for the detection of diazinon (DZN) on a cyclic olefin copolymer (COC) substrate. The aptasensor design was based on rolling circle amplification (RCA) technology and the use of self-assembled copper nanoparticles (CuNPs). A dual-function (DF) probe, capable of binding to circular DNA and an aptamer, was designed and immobilized on a COC-bottom 96-well plate. An aptamer was used for selective recognition of DZN, and the specific site of the aptamer that strongly reacted with DZN was successfully identified using circular dichroism (CD) analysis. In presence of DZN, the aptamer and DZN formed a strong complex, thus providing an opportunity for hybridization of the DF probe and circular DNA, thereby initiating an RCA reaction. Repetitive poly thymine (T) sequence with a length of 30-mer, generated in the RCA reaction, served as a template for the synthesis of fluorescent copper nanoparticles, emitting an orange fluorescence signal (at approximately 620 nm) proportional to the amount of RCA product, within 10 min under UV irradiation. The CuNP fluorescence was imaged and quantified using an image analysis software. A linear correlation of the fluorescence signal was confirmed in the DZN concentration range of 0.1-3 ppm, with a detection limit of 0.15 ppm. Adoption of a label-free detection method, utilizing RCA and fluorescent CuNPs on COC substrates, reduced the need for complex equipment and requirements for DZN analysis, thereby representing a simple and rapid sensing method circumventing the limitations of current complex and labor-intensive methods.

**Keywords:** diazinon, aptamer, rolling circle amplification, copper nanoparticle, fluorescent sensor, cyclic olefin copolymer

## 1. Introduction

Diazinon [O,O-diethyl O-(2-isopropyl-6-methylpyrimidin-4-yl) thiophosphate] (DZN) is an organophosphate pesticide (OP) that is widely used in agriculture and horticulture as an insecticide [1]. It inhibits acetylcholinesterase activity in the target organism, preventing neurotransmission [2]. Excess usage of DZN leads to increased residues in foods and can be highly toxic when ingested, causing symptoms, such as headache, nausea, vomiting, diarrhea, shortness of breath, and loss of consciousness [3,4]. Children are particularly vulnerable, since it affects the development of their brain and nervous system [5]. Therefore, despite the maximum residue limit of DZN being strictly established by the European Union for various foods [6], development of a simple and rapid method for determining the amount of residual DZN in food and environmental samples remains critical.

General quantification of OPs is conducted using chromato-

Tai-Yong Kim, Min-Cheol Lim, Min-Ah Woo*
Research Group of Food Safety and Distribution, Korea Food Research Institute (KFRI), Wanju, Korea
Tel: +82-63-219-9374; Fax: +82-63-219-9876
E-mail: mawoo@kfri.re.kr

Tai-Yong Kim
Department of Food Science and Technology, Jeonbuk National University, Jeonju, Korea

Ji Won Lim
The 4th R&D Institute, 6th Directorate, Agency for Defense Development, Daejeon, Korea

graphic techniques coupled with various detectors, such as high-performance liquid chromatography (HPLC) [7], thin layer chromatography (TLC) [8], and gas chromatography-mass spectrometry (GC-MS) [9]. Although these methods provide sensitive and accurate results, they are labor-intensive, time-consuming, and require complex sample preparation procedures, expensive analytical equipment, and skilled personnel. To overcome these challenges, various biosensors have been developed to detect OPs [10-13], among which, fluorescent sensors with easy manipulation and high sensitivity have proven successful [14-16]. Recently, our research group has reported a fluorescence resonance energy transfer-based fluorescent sensor, for the detection of pesticide in real food sample, with very simple and sensitive analytical properties [17].

Fluorescent copper nanoparticles (CuNPs), in particular, can be synthesized simply and quickly using DNA with a specific nucleotide sequence as a template, and can be applicable in biosensors following a label-free detection method based on the advantages of high efficiency, high resistance to photobleaching, low biological toxicity, and large Stokes shift (approximately 270 nm) [18]. The large Stokes shift eliminates the spectral overlap between absorption and emission and reduces interference, providing a strong fluorescence signal with a high signal-to-noise ratio, which is especially useful in multiple fluorescence applications, since it can excite different phosphors in the same sample [19]. DNA oligomers, which serve as the template for the synthesis of copper nanoparticles (CuNPs), can be amplified by rolling circle amplification (RCA) reactions under isothermal conditions, and eventually applied to biosensors [20,21]. The RCA method generates single-stranded DNA (ssDNA) to replicate numerous desired sequences and has been widely adopted as a strategy for signal amplification in various biosensors [22,23]. To identify a ssDNA amplified through RCA, sequence-specific labeling is performed [24-26]. A new label-free strategy has also been developed for CuNP synthesis, using thymine repeats as a template, and has been shown to be applicable in the detection of target DNA [27].

Unlike conventional chromatography-based methods for chemical detection, biosensors are simple, rapid, and highly efficient detection platforms. Chip-based sensors are popular owing to their low reagent consumption, simple procedure, multiple analyses, and high portability, and have been successfully employed in numerous studies [28-30]. RCA is an isothermal amplification, and is used for highly sensitive detection, offering an advantage for application in point-of-care testing (POCT) platforms [31-34]. Previously, we had demonstrated the application of a portable RCA chip for POCT of hazardous chemical analytes [35,36]. However, to use RCA technology in a probe-immobilized chip and further extend it to the POCT platforms, it would be necessary to select and use appropriate substrates that are compatible with biochemical reactions (*e.g.* RCA), have good durability, can be readily manufactured, exhibit chemical resistance, and have optical transparency. Considering these requirements, the cyclic olefin copolymer (COC) was proposed as a suitable material [37,38]. DNA oligonucleotide probes are easily immobilized on the COC surface through UV irradiation without surface modification [39], making it well suited for the fabrication of a chip-based biosensor [40-43].

In this study, a label-free fluorescence detection method, combining isothermal amplification technology and CuNP synthesis, was developed for the selective detection of DZN on COC substrates. To this end, a dual-function (DF) probe that can be readily immobilized on the non-modified COC surface and can bind to the aptamer for DZN as well as circular DNA for RCA reaction was elaborately designed. In presence of DZN, DF probe bound to the circular DNA and induced an RCA reaction, producing repetitive thymine. CuNPs could be rapidly synthesized on the poly thymine template, and a quantifiable fluorescence signal could be imaged and subsequently analyzed. The conditions for synthesizing CuNPs from RCA products were optimized and various experimental conditions to maintain the optimal environment for each reaction step were established. Analytical utility of the proposed method was demonstrated based on the linear calibration curve obtained using a standard solution of DZN.

## 2. Materials and methods

### 2.1. Chemicals and reagents

Information regarding the chemicals and reagents used in this study is listed in Table S1.

### 2.2. Circular dichroism spectroscopy for diazinon-specific aptamer

To identify an optimal hybridization site on the diazinon (DZN)-specific aptamer for a dual-function (DF) probe, formational changes in the aptamer complex were analyzed using a circular dichroism (CD) spectrometer (J-715, JASCO, Tokyo, Japan). Four individual complementary DNAs (cDNAs) were prepared for hybridization to the aptamer (Table S2). Three types of test samples were prepared for CD analysis (A, B, and C) in 1× binding buffer (BB). For sample type A, solutions of the aptamer and cDNA were mixed and the mixed sample was sequentially incubated at 88°C for 5 min, 30°C for 30 min, and subsequently cooled to 25°C. For sample type B, DZN was added to sample A, followed by incubation at 30°C for 30 min. For sample

type C, the aptamer solution was mixed with the DZN solution, incubated at 30°C for 30 min, and each cDNA solution was added without further incubation. The final concentrations of aptamer, cDNA, and DZN in all test solutions for CD analysis were 0.5 μM, 1 μM, and 1 ppm, respectively. CD spectra were obtained in the range of 220-340 nm at a scanning speed of 100 nm/min.

### 2.3. Sequence optimization of dual-function probe

Two DF probes were tested to identify the spacer length between the chip-binding site poly thymine (T)10-poly cytosine (C)10 and the dual-function site of the DF probe. The DF probe A, with a 9-mer spacer, and DF probe B, with an 11-mer spacer, were dissolved in distilled water (DW) to achieve various concentrations (0, 0.1, 0.5, 5, and 10 μM). Each DF probe solution (20 μL) was loaded onto a COC-bottom 96-well plate and dried at 25°C for 16 h and at 65°C for 30 min in a dry oven. Once the solutions were completely dried, the COC-bottom 96-well plate was exposed to 254 nm UV light with power of 3 $mW/cm^2$ for 30 min in an XL-1000 UV Crosslinker (Spectronics Corporation, Westbury, NY, USA) to immobilize the DF probes on the COC surface, followed by a single wash with 0.1× standard saline citrate (SSC) buffer containing 0.1% sodium dodecyl sulfate (SDS) for 10 min, and finally rinsed four times with DW. 20 μL of 0.5 μM circular DNA solution in hybridization buffer (Sigma) was added to the wells and incubated at 30°C for 1 h, followed by similar washes as mentioned above. Next, 30 μL of RCA solution (1× buffer, 1 mM dNTP mixture, and 20 units of phi29 DNA polymerase) were added to the wells and incubated at 30°C for 2 h and at 65°C for 10 min. Thereafter, 20 μL of 5× SYBR Green II was added, and fluorescence intensity at 522 nm measured, with excitation at 480 nm, using a multi-mode microplate reader (SpectraMax i3x, Molecular Devices, Sunnyvale, CA, USA) after incubation at 25°C for 10 min.

### 2.4. UV-based immobilization of oligonucleotides on COC substrate

DF probe B was fixed to the COC bottom of the 96-well plate by modifying a previously reported method [39]. To ensure immobilization of the DF probe on the COC substrate, various concentrations (0, 0.5, 1, 5, 10, and 20 μM) of DF probe B, modified with cyanine (cy3) dye at the 3' end, were prepared in DW, and 20 μL of the same loaded into each well. The samples were sequentially dried, and UV irradiated for 30 min. Standard washes with 0.1% SDS in 0.1× SSC buffer and DW were conducted next. The experiment was repeated five times, and fluorescence intensity at 575 nm was measured, with excitation at 530 nm, using a microplate reader.

### 2.5. Synthetic optimization and characterization of DNA-templated CuNP

To optimize CuNP synthesis, the optimum reaction time and concentrations of MOPS buffer, $CuSO_4$ solution, and sodium ascorbate (ASC) solution were individually tested. Prior to this experiment, circular DNA template was prepared for the RCA reaction [25] (Fig. S1). The 40 μL RCA reaction mixture contained 400 nM DF probe B, 200 nM circular DNA, 1× RCA buffer, 1.25 mM dNTP mixture, and 30 units of phi29 DNA polymerase. The RCA reaction was performed at 30°C for 2 h and inactivated at 65°C for 10 min. First, to optimize the concentration of MOPS buffer (10 mM MOPS, 150 mM NaCl, pH 7.6) for CuNP synthesis, 40 μL of RCA product solution was mixed with various concentrations of MOPS buffer (0, 1, 2, and 4×), 4 mM ASC, and 200 μM $CuSO_4$, and incubated at 25°C for 10 min. Subsequently, effects of ASC concentration (0.5, 1, 2, 3, 4, and 5 mM), $CuSO_4$ concentration (200, 400, 600, 800, 1000, and 1200 μM), and reaction time (from 0 to 2 h) were individually investigated. Fluorescence spectrum of the final reaction solution, for selecting the optimal concentrations of ASC and $CuSO_4$, was recorded with excitation at 350 nm, and fluorescence intensity of the final reaction solution at 620 nm was recorded for optimizing the CuNP synthesis time using a microplate reader with excitation at 350 nm.

Transmission electron microscopy (TEM) was performed to evaluate the morphological properties of CuNPs synthesized using the RCA product. Samples consisting of 400 nM DF probe B, 200 nM circular DNA, 1× RCA buffer, and 1.25 mM dNTP mixture were prepared with or without 30 units of phi29 DNA polymerase. The RCA reaction was conducted at 30°C for 1.5 h and inactivated at 65°C for 10 min (in EP tube). To synthesize CuNP, the RCA product solutions were mixed with 2 mM ASC, 0.5 mM $CuSO_4$, and 1× MOPS buffer, and incubated for 5 min in the dark. The prepared samples were imaged using TEM (Hitachi H-7650).

### 2.6. RCA test on COC substrate

To confirm the possibility of integrating the DZN detection method and COC substrate, fluorescence intensity of CuNPs was tested based on the amount of RCA product derived from the DF probe fixed to on the COC-bottom 96-well plate. First, 20 μM DF probe B was fixed to the COC plate as described in the UV-based immobilization of oligonucleotides on COC substrate section. Next, 20 μL of circular DNA of varying concentrations (0-2 μM) in hybridization buffer (Sigma) was added at 30°C for 1 h. After washing the wells of the plate, 40 μL of RCA solution containing 1× RCA buffer, 1 mM dNTP mixture, and 30 units of phi29 DNA polymerase were added to each

well, incubated at 30°C for 2 h, and inactivated at 65°C for 10 min. The synthesis of CuNPs was performed at 25°C for 10 min by adding 4 mM ASC and 1 mM $CuSO_4$ to the RCA product solution, and fluorescence intensity at 620 nm was measured by a microplate reader using excitation at 350 nm.

### 2.7. Linearity and selectivity test of the proposed method of DZN detection on COC substrate

20 µL of 20 µM DF probe B solution was immobilized to each well of the COC-bottom 96-well plate by UV irradiation. Following this, 20 µL of 20 µM aptamer solution in hybridization buffer was added and incubated at 34°C for 1 h with gentle shaking. Subsequently, DZN solutions of various concentrations, dissolved in 1× BB, were added to each well and incubated at 30°C for 1 h with gentle shaking. For the hybridization reaction of free DF probe B fixed on COC substrate with circular DNA, 20 µL of 2 µM circular DNA solution dissolved in hybridization buffer was added to each well and incubated at 30°C for 1 h with gentle shaking. Subsequently, the RCA reaction was performed at 30°C for 5 h after 40 µL of RCA solution was added to each well, followed by incubation at 65°C for 10 min. To synthesize CuNPs using RCA product, 4 mM ASC and 1 mM $CuSO_4$ were added to each well and incubated at 25°C for 10 min in the dark. The plate was imaged using an Alliance Mini HD9 system (UVITEC, USA) under UV irradiation conditions, and fluorescence of the CuNPs was quantified using an image analysis software (Nine-Alliance Q9). Standard washes were performed, except for the CuNP synthesis reaction, in order to maintain the optimal buffer conditions for each reaction step. Each experiment was repeated thrice to generate a standard curve. To evaluate selectivity of the proposed method, 4 ppm of four pesticides, including DZN, were prepared in 1× BB and assessed in the same way as described above for the linearity test. Each experiment was repeated thrice.

## 3. Results and Discussion

### 3.1. Label-free aptasensor design for diazinon detection on cyclic olefin copolymer substrate

The detection method developed for diazinon (DZN) on a cyclic olefin copolymer (COC) substrate was designed by combining a DZN-specific aptamer, rolling circle amplification (RCA) technology, and self-assembled copper nanoparticles (CuNPs). A schematic illustration of the proposed detection method is shown in Fig. 1; a series of reactions for DZN detection was performed on a COC substrate, which allowed washing as well as performance of each reaction under optimal buffer conditions. For this purpose, a 96-well plate containing COC film on the bottom was adopted as an analysis tool. Using this experimental setup, integration of this method into compact detection platforms, such as a DNA chip or microfluidic chip made of COC, was evaluated.

DF probes were immobilized onto the COC substrate through UV irradiation [39]. As shown in Table S2, the DF probe consisted of a poly thymine (T)10-poly cytosine (C)10 site at the 5' end for UV immobilization, a spacer in the middle, and a dual binding site (that can bind to the DZN-specific aptamer or circular DNA) at the 3' end. Functionally, the DF probe not only captures the aptamer, but also acts as a primer for initiating the RCA reaction by binding to circular DNA. Therefore, the DF probe fixed on the bottom of the COC well plate can hybridize the aptamer to form a partial double complex. If DZN is

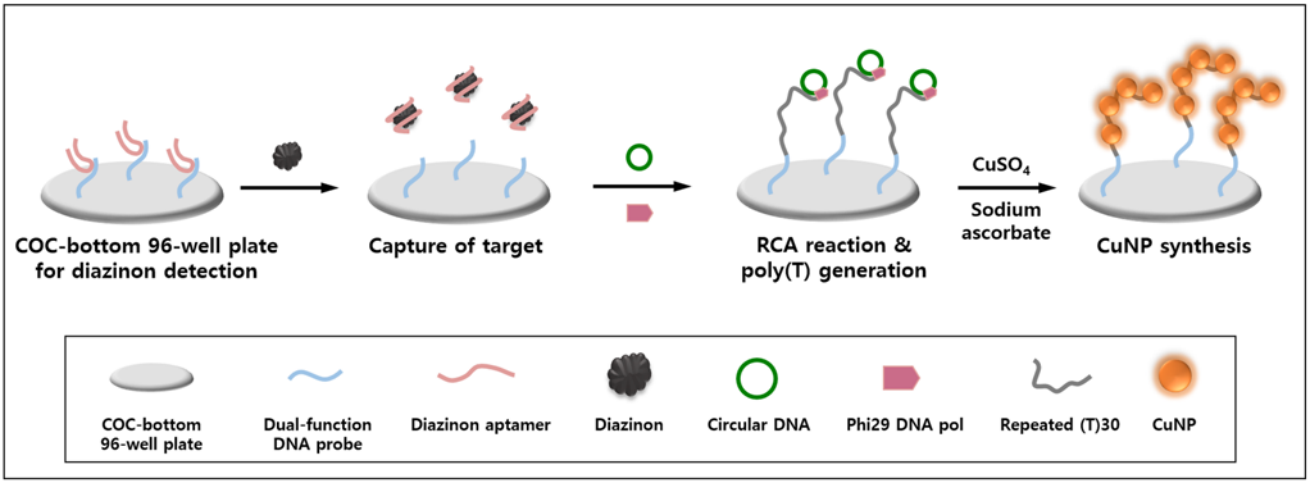


**Fig. 1.** Schematic representation of the label-free fluorescence detection method, based on isothermal amplification technology, for detecting diazinon on COC substrate.

present in the assay sample, the DF probe becomes free as the aptamer gets detached from the DF probe, forming a strong complex with DZN. The free DF probe is hybridized with circular DNA to initiate the RCA reaction and produces ssDNA as RCA products, proportional to the amount of DZN. The ssDNA has a repetitive sequence in which the (T)30 sequence, complementary to circular DNA, serves as a template for the synthesis of fluorescent CuNPs [27]. The fluorescent CuNPs were synthesized 10 min after the addition of $CuSO_4$ and sodium ascorbate (ASC) without the requirement of an additional labeling process, resulting in fluorescence emission at 620 nm, proportional to the amount of DZN under UV light.

### 3.2. Design and verification of a dual-function probe

The ability of a DF probe to bind to a circular DNA as well as a DZN-specific aptamer plays an important role in our detection strategy. Since the DF probe consists of cDNA toward the aptamer, we identified the aptamer site that sensitively and selectively reacts with DZN using CD analysis. Four types of cDNA candidates that can bind to different sites (sites 1-4) of the aptamer were synthesized such that all cDNAs were 10-mer (Fig. 2A).

A schematic diagram for the binding sites of cDNAs to the aptamer are shown in Fig. 2A and the results of CD analysis are shown in Fig. 2B. Type A samples contained aptamer and each cDNA; type B had DZN added to the type A sample; type C was a sample in which the aptamer and DZN reacted first, and cDNA was added subsequently without an additional hybridization reaction. Thus, sample type A formed a duplex with the aptamer and cDNA, and sample type C formed an aptamer-DZN complex. When reactivity between the aptamer and DZN was low, the spectrum of sample B was skewed toward that of sample

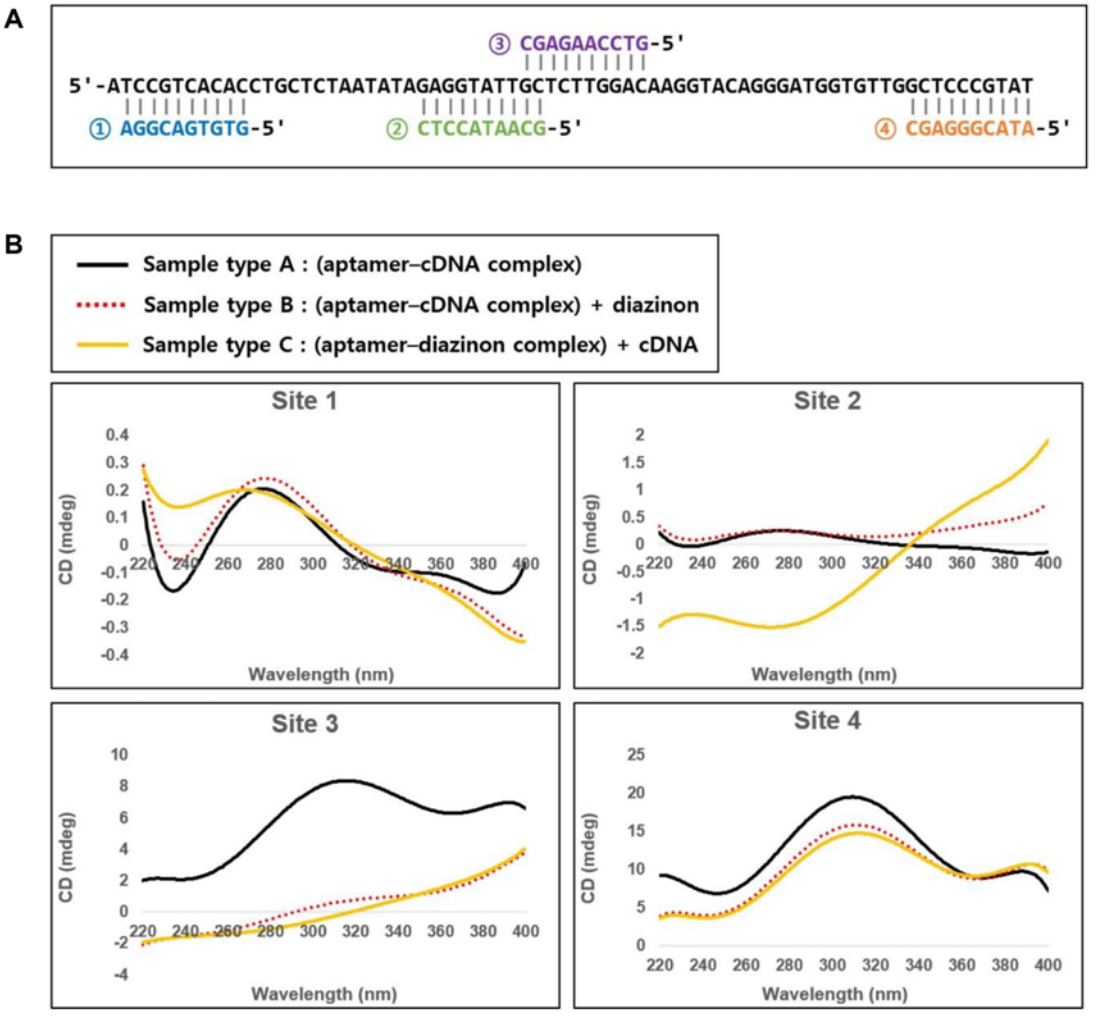


**Fig. 2.** Conformational changes in the aptamer following interaction with cDNA and diazinon. (A) Schematic diagram of the aptamer (72-mer)-binding site of four cDNAs (①-④). (B) Circular dichroism (CD) spectra for the three sample combinations. Final concentration of diazinon was 1 ppm.

A, whereas when the reactivity was high, the spectrum of sample B skewed toward that of sample C. Aptamer sites 1 and 2 were found to have a stronger tendency to bind cDNA than DZN, since the corresponding spectral patterns of sample types A and B were similar. In other words, aptamer sites 1 and 2 had low reactivity for DZN. On the other hand, aptamer sites 3 and 4 were highly reactive for DZN, since types B and C exhibited similar spectral patterns. In case of site 3, in particular, the distinct spectral pattern difference between the aptamer-cDNA complex (type A) and aptamer-DZN complex (type C) indicated a large difference between the three-dimensional structures of the two complexes. Therefore, among the four candidate sites, site 3 was considered to be the most suitable for DF probe design, and hence, was ultimately selected.

Another important factor to consider when designing a DF probe is the spacer length. The spacer between the chip-binding site and dual-function site of the DF probe serves to reduce steric hindrance in hybridization reactions with aptamer or circular DNA. Therefore, RCA efficiency on the COC substrate was tested based on the DF probe spacer length. DF probes A and B with spacer lengths of 9- and 11-mer, respectively, were immobilized on the COC-bottom of the 96-well plate, followed by a hybridization reaction with the same amount of circular DNA, and staining with SYBR green dye. As shown in Fig. S2, the fluorescence intensity increased, in both cases, as the DF probe concentration increased. Since the difference between DF probes A and B was negligible, spacer length was considered to not affect the immobilization efficiency significantly. The results from 2 h RCA reaction under the same conditions are shown in Fig. 3B. In case of DF probe A with a 9-mer spacer, the RCA product gradually increased in yield as the concentration of DF probe A increased from 0 to 0.5 μM; however, it decreased thereafter. In case of DF probe B, with an 11-mer spacer, the RCA product consistently increased as the DF probe B concentration increased from 0 to 10 μM.

In addition, the RCA efficiency of DF probe B was significantly higher than that of DF probe A (Fig. 3A), suggesting that a spacer length ≥ 11-mer would be required to immobilize the probe on the COC substrate, and to serve as a primer for the RCA reaction without steric hindrance. Therefore, an additional immobilization reaction on the COC substrate was performed using the 11-mer DF probe B conjugated with cyanine (cy3) dye at the 3' end. This confirmed that the fluorescence intensity increased as the DF probe B concentration increased (0-20 μM; Fig. 3C), hence suggesting a proportional increase in the amount of DF probe B immobilized on the COC substrate. Based on

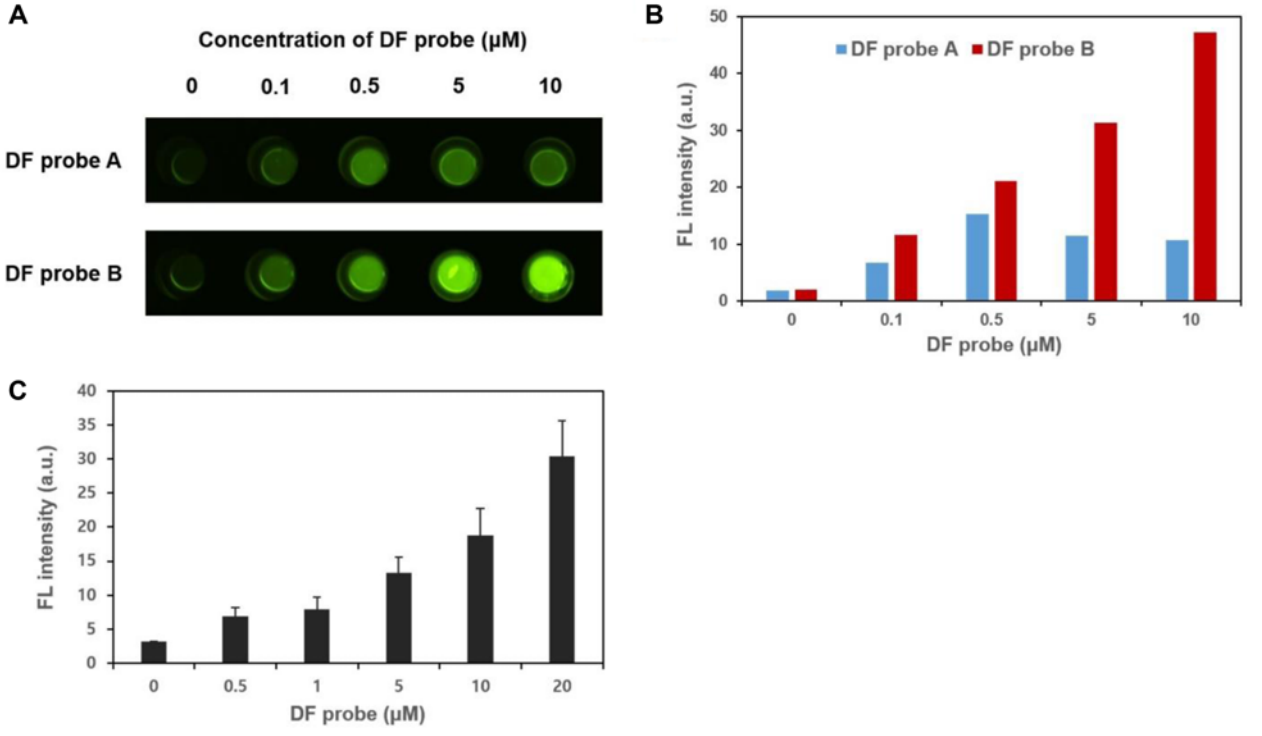


**Fig. 3.** SYBR green (A) fluorescence image and (B) quantification for testing RCA efficiency on COC substrate based on spacer sequence length of the DF probe. The excitation and emission wavelengths for fluorescence (FL) measurement of SYBR green dye were 480 and 522 nm, respectively. (C) Immobilization result for each concentration of DF probe B on COC-bottom 96-well plate (n = 5). The excitation and emission wavelengths for fluorescence measurement of cy3 dye were 530 and 575 nm, respectively.

the results, 20 μM was chosen as the optimal concentration of DF probe for the fixation reaction.

### 3.3. Optimization and verification of CuNP synthesis based on RCA product as a template

To optimize the synthesis of CuNPs using the RCA product as a template, the optimal concentrations of MOPS buffer, $CuSO_4$ solution and ASC solution, and optimal CuNP synthesis time were explored. Since the RCA product contained RCA buffer and dNTPs, the CuNP synthesis conditions were crucial. In case of MOPS buffer effect, CuNP synthesis efficiency was the highest when DW was used instead of MOPS buffer (Fig. 4A). When the MOPS buffer concentration was fixed at 0×, the effect of ASC concentration was tested from 0.5 to 5 mM; CuNP synthesis efficiency was the highest at 4 mM (Fig. 4B). The effect of $CuSO_4$ concentration was investigated from 200 to 1,200 μM, with MOPS buffer at 0× and ASC concentration at 4 mM; the most efficient CuNP synthesis was observed at 1,000 μM $CuSO_4$ (Fig. 4C).

Reaction time (from 0 to 120 min) was investigated under the optimal conditions of the previous three factors. As time progressed, the fluorescence of CuNPs gradually decreased, and a plateau was confirmed from 10 to 20 min. The optimal time for CuNP synthesis was determined as 10 min (Fig. 4D).

TEM was performed for analyzing the morphology of CuNPs synthesized using the RCA product as a template. Results confirmed that a 3-5 nm spherical CuNP was synthesized from the sample that underwent RCA reaction for 90 min (Fig. 5A, left). The result was consistent with that reported in previous studies, where CuNPs had been synthesized using (T)30 ssDNA as a template [44]. In the negative sample, to which phi29 DNA polymerase had not been added, the RCA reaction was not induced and CuNP was not formed (Fig. 5A, right). To identify any correlation between the fluorescence signal of CuNPs and the RCA product, the DF probe was first immobilized on a COC-

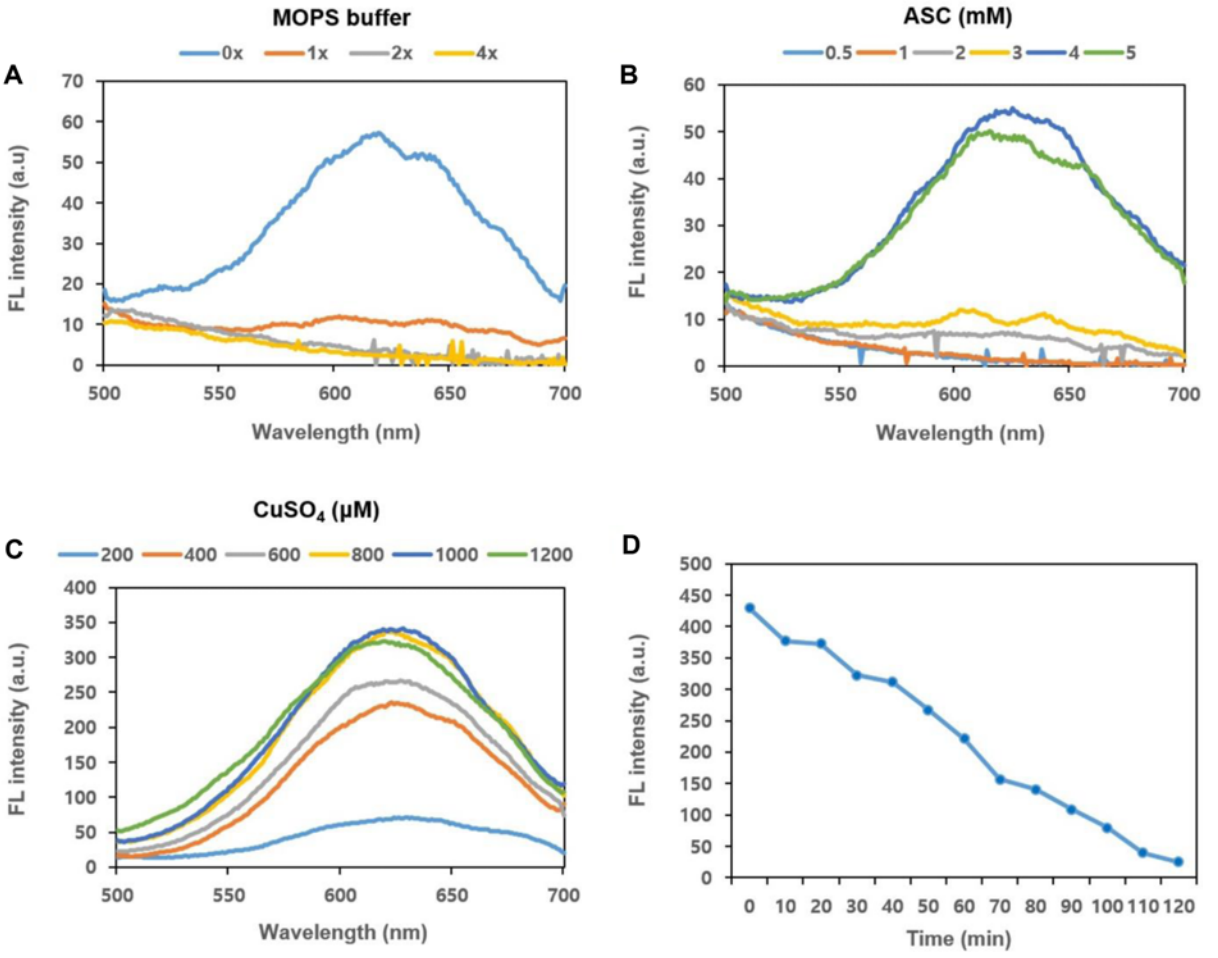


**Fig. 4.** Optimization of CuNP synthesis using the RCA product as template. (A) MOPS concentration, (B) sodium ascorbate concentration, (C) copper(II) sulfate concentration, and (D) reaction time. Excitation wavelength for all spectral results was 350 nm; for reaction time emission wavelength of 620 nm was selected under 350 nm excitation conditions.

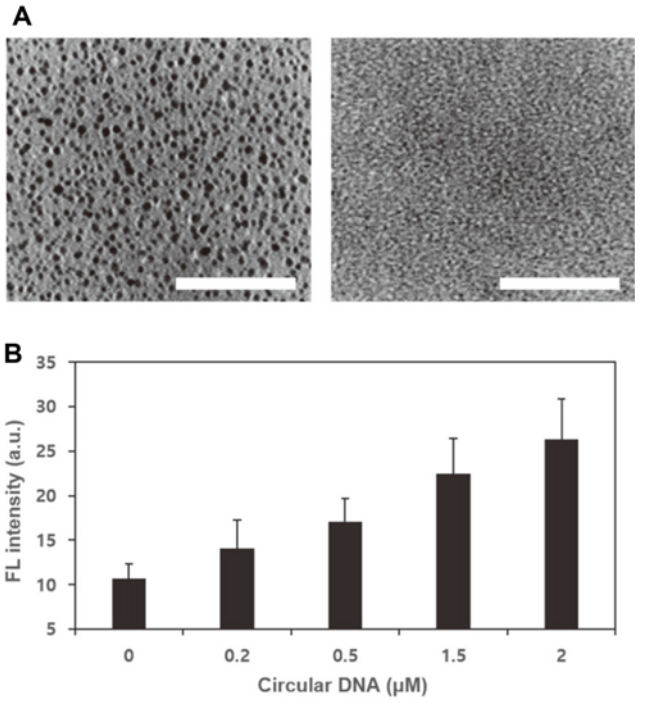


**Fig. 5.** (A) TEM images of CuNPs synthesized using the RCA product (left), and of negative control in which no RCA reaction was induced (right). (B) A graph of the relationship between CuNP fluorescence (FL) intensity at 620 nm versus the concentration of circular DNA added for RCA reaction (n = 5). Length of the scale bars is 100 nm.

bottom 96-well plate, and various concentrations of circular DNA (from 0 to 2.0 μM) were added and hybridized, followed by a subsequent 2 h RCA reaction. CuNP synthesis was induced for 10 min in each well after the RCA reaction was completed, and a fluorescence intensity was recorded at 620 nm, with excitation at 350 nm. Fluorescence increased as the concentration of circular DNA increased (Fig. 5B). The experiment confirmed that an increase in the amount of RCA product resulted in an increase in the amount of (T)30 used as a template for CuNP synthesis, and finally, in increased fluorescence of CuNPs.

### 3.4. Verification of the proposed method for detection of diazinon

Sensitivity and selectivity toward target substances are key factors for evaluating the performance of biosensors. Performance of the proposed method for DZN detection was evaluated under optimal conditions selected from previous experiments. First, to evaluate the sensitivity of the proposed method, seven samples containing different DZN concentrations (0-5 ppm) in 1× BB were prepared and tested in triplicate. To increase the applicability of this detection method to resource-constrained field analysis, the final fluorescence signal of the well plate was captured as an image using the Alliance Mini HD9 system (UVITEC, USA; Fig. 6A).

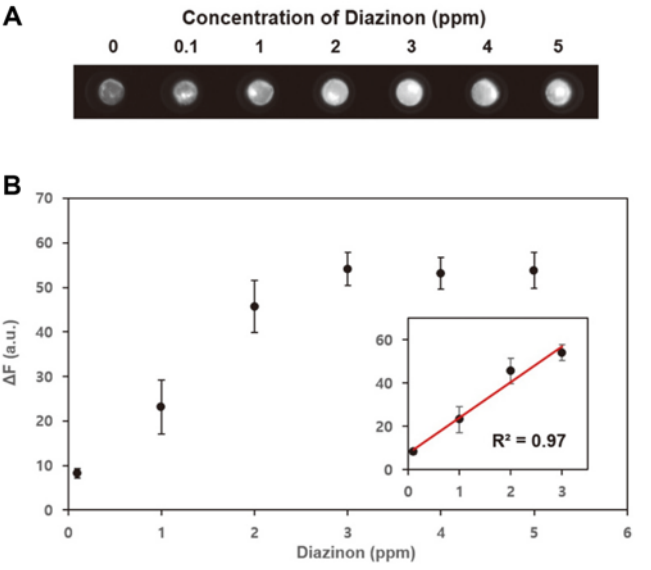


**Fig. 6.** DZN sample analysis using the proposed method. (A) Fluorescence image from the COC-bottom 96-well plate. (B) Standard curve for ΔF value ($F-F_0$) versus DZN concentration obtained based on image A (n = 3). Inset: linear relationship between the ΔF value variations and the DZN concentration.

As the concentration of DZN increased from 0 to 5 ppm, the fluorescence intensity of CuNPs gradually increased, and was visually identified; fluorescence intensity, however, saturated after 3 ppm. To obtain a standard curve for the $F-F_0$ (ΔF) value versus DZN concentration, fluorescence intensity of the captured image was quantified using the image analysis software (Nine-Alliance Q9) of the Alliance Mini HD9 system. F is the fluorescence intensity of the sample in which DZN is present, and $F_0$ is the fluorescence intensity of the blank sample without DZN. The mean ΔF values of CuNPs according to DZN concentration (0.1, 1, 2, 3, 4, and 5 ppm) were 8.26 ± 1.03, 23.14 ± 6.1, 45.68 ± 5.87, 54.12 ± 3.67, 53.14 ± 3.52, and 53.89 ± 4.05, respectively. The standard curve (Fig. 6B) indicated the linearity from 0.1 to 3 ppm of DZN concentration. The correlation equation was $y = 16.49 x + 7.66$ and the $R^2$ value was determined to be 0.97. The limit of detection (LOD) for DZN was calculated to be 0.15 ppm, using the following formula: LOD = 3.3 × (SD/S), where SD and S are the standard deviation of y-intercepts and slope of the calibration curve, respectively (n = 3).

In the case of other sensors developed previously, the LOD values of the aptamer-based sensors are in the range of $0.01 \times 10^{-3}$ - $6.7 \times 10^{-3}$ ppm [45-49] and the enzyme-based sensors are in the range of $0.06 \times 10^{-3}$ - $170 \times 10^{-3}$ ppm [50-56], so that the average LOD value of the aptamer-based sensors is 14 times lower than that of the enzyme-

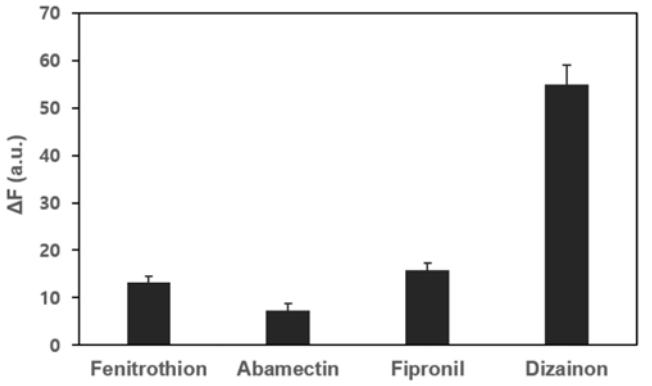


**Fig. 7.** Selectivity of the proposed assay for DZN (n = 3).

based sensors. While the previously developed aptamer-based sensor adopted a solution-based detection method, the newly developed method has the potential to be expanded to a detection platform capable of high-throughput screening because it used an immobilized surface-based detection method. Nevertheless, it is necessary to improve the sensitivity of our sensor compared to the existing sensors, and there is room for sensitivity improvement because our sensor has the advantage of using an aptamer that has a positive effect on detection sensitivity and selectivity compared to enzymes.

Selectivity of the proposed method for the detection of DZN was also evaluated. DZN, fenitrothion, abamectin, and fipronil were prepared at a concentration of 4 ppm each in 1× BB and tested thrice in the same manner as the above sensitivity test (Fig. 7). Unlike other pesticide samples, only the DZN sample showed high ΔF values. The mean values of ΔF for fenitrothion, abamectin, fipronil, and DZN were 13.19 ± 1.34, 7.21 ± 1.59, 15.87 ± 1.5, and 54.9 ± 4.18, respectively. The results confirmed that the proposed detection method is selective to DZN detection.

## 4. Conclusion

In this study, we described a label-free fluorescent aptasensor, based on RCA and self-assembled CuNPs, to detect DZN on a COC substrate. A recent report featuring the properties of DZN-specific aptamer [45] was referred to while devising this detection strategy. The DF probe was designed for efficient RCA reactions, enabling a series of reactions to detect DZN on non-modified COC substrates. A strong and selective aptamer-DZN complex induced an RCA reaction on the COC substrate and produced an ssDNA product with repetitive (T)30 sequence. The RCA product could act as a template for fluorescent CuNP synthesis and, within 10 min, was converted to a fluorescence signal proportional to DZN concentration. For quantitative DZN analysis, the fluorescence signal was captured as a digital image and quantified using an image analysis software. The DZN analysis method confirmed linearity of the fluorescence signal of DZN (ranging from 0.1 to 3 ppm), and identified the detection limit as 0.15 ppm. The current study provided a simple and selective DZN detection strategy involving UV-based DNA probe immobilization on a non-modified COC substrate, target-specific aptamer, optimized DF probe, and self-assembled CuNPs by isothermal RCA. This novel method for the detection of DZN was found to be efficient, with minimized use of expensive and complex equipment compared to conventional chromatography-based methods, thus proving to be an ideal detection strategy for chip-based biosensors made of COC substrates while allowing for its further exploitation for the simultaneous detection of multiple targets.

## Acknowledgments

The study was supported by the Korea Food Research Institute research program, funded by the Ministry of Science and ICT of South Korea.
The authors declare no conflict of interest.
Neither ethical approval nor informed consent was required for this study.

## Electronic Supplementary Material (ESM)

The online version of this article (doi: 10.1007/s12257-021-0220-0) contains supplementary material, which is available to authorized users.

## References

1. National Pesticide Information Center, Diazinon general fact sheet. http://npic.orst.edu/factsheets/Diazgen.html.
2. Díaz-Resendiz, K. J. G., P. C. Ortiz-Lazareno, C. E. Covantes-Rosales, A. M. Trujillo-Lepe, G. A. Toledo-Ibarra, G. H. Ventura-Ramón, and M. I. Girón-Pérez (2019) Effect of diazinon, an organophosphate pesticide, on signal transduction and death induction in mononuclear cells of Nile tilapia fish (*Oreochromis niloticus*). *Fish Shellfish Immunol.* 89: 12-17.
3. Sidhu, G. K., S. Singh, V. Kumar, D. S. Dhanjal, S. Datta, and J. Singh (2019) Toxicity, monitoring and biodegradation of organophosphate pesticides: a review. *Crit. Rev. Environ. Sci. Technol.* 49: 1135-1187.
4. U.S. Department of Health and Human Services (2008) Toxicological profile for diazinon. https://www.atsdr.cdc.gov/toxprofiles/tp86.pdf.
5. Eskenazi, B., A. Bradman, and R. Castorina (1999) Exposures of children to organophosphate pesticides and their potential adverse

health effects. *Environ. Health Perspect.* 107 supple: 409-419.
6. The European Commission 2013, Commission Regulation (EU) No 834/2013. http://data.europa.eu/eli/reg/2013/834/oj.
7. Harshit, D., K. Charmy, and P. Nrupesh (2017) Organophosphorus pesticides determination by novel HPLC and spectrophotometric method. *Food Chem.* 230: 448-453.
8. Skowron, M., R. Zakrzewski, and W. Ciesielski (2016) Application of image analysis technique for the determination of organophosphorus pesticides by thin-layer chromatography. *JPC-J. Planar Chromat.* 29: 221-226.
9. Xie, J., T. Liu, G. Song, Y. Hu, and C. Deng (2013) Simultaneous analysis of organophosphorus pesticides in water by magnetic solid-phase extraction coupled with GC-MS. *Chromatographia.* 76: 535-540.
10. Ebrahimi, B., S. A. Shojaosadati, and S. M. Mousavi (2010) Evaluation and optimization of factors affecting the performance of a flow-through system based on immobilized acetylcholineesterase as a biosensor. *Biotechnol. Bioprocess Eng.* 15: 383-391.
11. He, L., Z. W. Jiang, W. Li, C. M. Li, C. Z. Huang, and Y. F. Li (2018) *In situ* synthesis of gold nanoparticles/metal-organic gels hybrids with excellent peroxidase-like activity for sensitive chemiluminescence detection of organophosphorus pesticides. *ACS Appl. Mater. Interfaces.* 10: 28868-28876.
12. Wu, Y., L. Jiao, W. Xu, W. Gu, C. Zhu, D. Du, and Y. Lin (2019) Polydopamine-capped bimetallic AuPt hydrogels enable robust biosensor for organophosphorus pesticide detection. *Small.* 15: e1900632.
13. Yang, T., J. Doherty, H. Guo, B. Zhao, J. M. Clark, B. Xing, R. Hou, and L. He (2019) Real-time monitoring of pesticide translocation in tomato plants by surface-enhanced Raman spectroscopy. *Anal. Chem.* 91: 2093-2099.
14. Yan, X., H. Li, T. Hu, and X. Su (2017) A novel fluorimetric sensing platform for highly sensitive detection of organophosphorus pesticides by using egg white-encapsulated gold nanoclusters. *Biosens. Bioelectron.* 91: 232-237.
15. Chen, J., X. Chen, Q. Huang, W. Li, Q. Yu, L. Zhu, T. Zhu, S. Liu, and Z. Chi (2019) Amphiphilic polymer-mediated aggregation-induced emission nanoparticles for highly sensitive organophosphorus pesticide biosensing. *ACS Appl. Mater. Interfaces.* 11: 32689-32696.
16. Ashrafi Tafreshi, F., Z. Fatahi, S. F. Ghasemi, A. Taherian, and N. Esfandiari (2020) Ultrasensitive fluorescent detection of pesticides in real sample by using green carbon dots. *PLoS One.* 15: e0230646.
17. Kim, T. Y., J. W. Lim, M. C. Lim, N. E. Song, and M. A. Woo (2020) Aptamer-based fluorescent assay for simple and sensitive detection of fipronil in liquid eggs. *Biotechnol. Bioprocess Eng.* 25: 246-254.
18. Qing, Z., A. Bai, S. Xing, Z. Zou, X. He, K. Wang, and R. Yang (2019) Progress in biosensor based on DNA-templated copper nanoparticles. *Biosens. Bioelectron.* 137: 96-109.
19. He, T., Y. Wang, X. Tian, Y. Gao, X. Zhao, A. C. Grimsdale, X. Lin, and H. Sun (2016) An organic dye with very large Stokes-shift and broad tunability of fluorescence: potential two-photon probe for bioimaging and ultra-sensitive solid-state gas sensor. *Appl. Phys. Lett.* 108: 011901.
20. Ali, M. M., F. Li, Z. Zhang, K. Zhang, D. K. Kang, J. A. Ankrum, X. C. Le, and W. Zhao (2014) Rolling circle amplification: a versatile tool for chemical biology, materials science and medicine. *Chem. Soc. Rev.* 43: 3324-3341.
21. Yue, S., Y. Li, Z. Qiao, W. Song, and S. Bi (2021) Rolling circle replication for biosensing, bioimaging, and biomedicine. *Trends Biotechnol.* 1160-1172.
22. Liu, C., J. Han, L. Zhou, J. Zhang, and J. Du (2020) DNAzyme-based target-triggered rolling-circle amplification for high sensitivity detection of microRNAs. *Sensors (Basel).* 20: 2017.
23. Chaibun, T., J. Puenpa, T. Ngamdee, N. Boonapatcharoen, P. Athamanolap, A. P. O'Mullane, S. Vongpunsawad, Y. Poovorawan, S. Y. Lee, and B. Lertanantawong (2021) Rapid electrochemical detection of coronavirus SARS-CoV-2. *Nat. Commun.* 12: 802.
24. Wang, D., L. Hu, H. Zhou, E. S. Abdel-Halim, and J. J. Zhu (2013) Molecular beacon structure mediated rolling circle amplification for ultrasensitive electrochemical detection of microRNA based on quantum dots tagging. *Electrochem. Commun.* 33: 80-83.
25. Kim, T. Y., M. C. Lim, M. A. Woo, and B. H. Jun (2018) Radial flow assay using gold nanoparticles and rolling circle amplification to detect mercuric ions. *Nanomaterials (Basel).* 8: 81.
26. Jia, Y., F. Sun, N. Na, and J. Ouyang (2019) Detection of p53 DNA using commercially available personal glucose meters based on rolling circle amplification coupled with nicking enzyme signal amplification. *Anal. Chim. Acta.* 1060: 64-70.
27. Park, K. W., C. Y. Lee, B. S. Batule, K. S. Park, and H. G. Park (2018) Ultrasensitive DNA detection based on target-triggered rolling circle amplification and fluorescent poly(thymine)-templated copper nanoparticles. *RSC Adv.* 8: 1958-1962.
28. Wang, X., J. Sun, J. Tong, X. Guan, C. Bian, and S. Xia (2018) Paper-based sensor chip for heavy metal ion detection by SWSV. *Micromachines (Basel).* 9: 150.
29. Patil, S. B., D. S. Dheeman, M. A. Al-Rawhani, S. Velugotla, B. Nagy, B. C. Cheah, J. P. Grant, C. Accarino, M. P. Barrett, and D. R. S. Cumming (2018) An integrated portable system for single chip simultaneous measurement of multiple disease associated metabolites. *Biosens. Bioelectron.* 122: 88-94.
30. Heo, N. S., S. Y. Oh, M. Y. Ryu, S. H. Baek, T. J. Park, C. Choi, Y. S. Huh, and J. P. Park (2019) Affinity peptide-guided plasmonic biosensor for detection of noroviral protein and human norovirus. *Biotechnol. Bioprocess Eng.* 24: 318-325.
31. Goo, N. I. and D. E. Kim (2016) Rolling circle amplification as isothermal gene amplification in molecular diagnostics. *Biochip J.* 10: 262-271.
32. Hernández-Neuta, I., I. Pereiro, A. Ahlford, D. Ferraro, Q. Zhang, J. L. Viovy, S. Descroix, and M. Nilsson (2018) Microfluidic magnetic fluidized bed for DNA analysis in continuous flow mode. *Biosens. Bioelectron.* 102: 531-539.
33. Garbarino, F., G. A. S. Minero, G. Rizzi, J. Fock, and M. F. Hansen (2019) Integration of rolling circle amplification and optomagnetic detection on a polymer chip. *Biosens. Bioelectron.* 142: 111485.
34. Ciftci, S., F. Neumann, S. Abdurahman, K. S. Appelberg, A. Mirazimi, M. Nilsson, and N. Madaboosi (2020) Digital rolling circle amplification-based detection of Ebola and other tropical viruses. *J. Mol. Diagn.* 22: 272-283.
35. Lim, J. W., T. Y. Kim, S. W. Choi, and M. A. Woo (2019) 3D-printed rolling circle amplification chip for on-site colorimetric detection of inorganic mercury in drinking water. *Food Chem.* 300: 125177.
36. Lim, J. W., T. Y. Kim, M. C. Lim, S. W. Choi, and M. A. Woo (2020) Portable pumpless 3D-printed chip for on-site colorimetric screening of Hg2+ in lake water. *Biochip J.* 14: 169-178.
37. Nunes, P. S., P. D. Ohlsson, O. Ordeig, and J. P. Kutter (2010) Cyclic olefin polymers: emerging materials for lab-on-a-chip applications. *Microfluid. Nanofluid.* 9: 145-161.
38. Berenguel-Alonso, M., M. Sabés-Alsina, R. Morató, O. Ymbern, L. Rodríguez-Vázquez, O. Talló-Parra, J. Alonso-Chamarro, M. Puyol, and M. López-Béjar (2017) Rapid prototyping of a cyclic olefin copolymer microfluidic device for automated oocyte culturing. *SLAS Technol.* 22: 507-517.
39. Sun, Y., I. Perch-Nielsen, M. Dufva, D. Sabourin, D. D. Bang, J. Høgberg, and A. Wolff (2012) Direct immobilization of DNA probes on non-modified plastics by UV irradiation and integration in microfluidic devices for rapid bioassay. *Anal. Bioanal. Chem.*

402: 741-748.
40. Sung, D., D. H. Shin, and S. Jon (2011) Toward immunoassay chips: facile immobilization of antibodies on cyclic olefin copolymer substrates through pre-activated polymer adlayers. *Biosens. Bioelectron*. 26: 3967-3972.
41. Prada, J., W. Lang, C. Cordes, and C. Harms (2018) A disposable, cyclo-olefin copolymer, RNA microfluidic sensor for bacteria detection. *Proceedings of 2018 IEEE Sensors*. October 28-31. New Delhi, India.
42. Bruijns, B., A. Veciana, R. Tiggelaar, and H. Gardeniers (2019) Cyclic olefin copolymer microfluidic devices for forensic applications. *Biosensors (Basel).* 9: 85.
43. Prada, J., C. Cordes, C. Harms, and W. Lang (2019) Design and manufacturing of a disposable, cyclo-olefin copolymer, microfluidic device for a biosensor. *Sensors (Basel).* 19: 1178.
44. Qing, Z., X. He, D. He, K. Wang, F. Xu, T. Qing, and X. Yang (2013) Poly(thymine)-templated selective formation of fluorescent copper nanoparticles. *Angew. Chem. Int. Ed.* 52: 9719-9722.
45. Jokar, M., M. H. Safaralizadeh, F. Hadizadeh, F. Rahmani, and M. R. Kalani (2017) Apta-nanosensor preparation and *in vitro* assay for rapid diazinon detection using a computational molecular approach. *J. Biomol. Struct. Dyn.* 35: 343-353.
46. Hassani, S., M. R. Akmal, A. Salek-Maghsoudi, S. Rahmani, M. R. Ganjali, P. Norouzi, and M. Abdollahi (2018) Novel label-free electrochemical aptasensor for determination of Diazinon using gold nanoparticles-modified screen-printed gold electrode. *Biosens. Bioelectron*. 120: 122-128.
47. Cheng, N., Y. Song, Q. Fu, D. Du, Y. Luo, Y. Wang, W. Xu, and Y. Lin (2018) Aptasensor based on fluorophore-quencher nano-pair and smartphone spectrum reader for on-site quantification of multi-pesticides. *Biosens. Bioelectron*. 117: 75-83.
48. Arvand, M. and A. A. Mirroshandel (2019) An efficient fluorescence resonance energy transfer system from quantum dots to graphene oxide nano sheets: application in a photoluminescence aptasensing probe for the sensitive detection of diazinon. *Food Chem.* 280: 115-122.
49. Talari, F. F., A. Bozorg, F. Faridbod, and M. Vossoughi (2021) A novel sensitive aptamer-based nanosensor using rGQDs and MWCNTs for rapid detection of diazinon pesticide. *J. Environ. Chem. Eng.* 9: 104878.
50. Zehani, N., S. V. Dzyadevych, R. Kherrat, and N. J. Jaffrezic-Renault (2014) Sensitive impedimetric biosensor for direct detection of diazinon based on lipases. *Front. Chem.* 2: 44.
51. Mulyasuryani, A. and S. Prasetyawan (2015) Organophosphate hydrolase in conductometric biosensor for the detection of organophosphate pesticides. *Anal. Chem. Insights.* 10: 23-27.
52. Wang, X., S. Dong, T. Hou, L. Liu, X. Liu, and F. Li (2016) Exonuclease I-aided homogeneous electrochemical strategy for organophosphorus pesticide detection based on enzyme inhibition integrated with a DNA conformational switch. *Analyst.* 141: 1830-1836.
53. Aghdas, B., P. Nahid, and B. Jalil (2019) Fabrication of choline oxidase enzyme-based nanobiosensor for the detection of diazinon and comparing its performance with the high performance liquid chromatography. *J. Appl. Res. Chem.* 12: 139-151.
54. Herrera, E. G., A. Bonini, F. Vivaldi, B. Melai, P. Salvo, N. Poma, D. Santalucia, A. Kirchhain, and F. Di Francesco (2019) A biosensor for the detection of acetylcholine and diazinon. *Proceedings of 2019 Annual International Conference of the IEEE Engineering in Medicine and Biology Society (EMBC).* July 23-27. Berlin, Germany.
55. Bagheri, N., A. Khataee, J. Hassanzadeh, and B. Habibi (2019) Sensitive biosensing of organophosphate pesticides using enzyme mimics of magnetic ZIF-8. *Spectrochim. Acta A Mol. Biomol. Spectrosc.* 209: 118-125.
56. Azis, T., C. Bijang, and A. Nurwahida (2020) Performance of platina electrode coated by butyrylcholinesterase-cellulose acetate-glutaraldehyde for diazinon detection. *Jurnal Riset Kimia.* 6: 106-111.